ELSEVIER

Biophysical Chemistry 56 (1995) 95–104

Biophysical Chemistry

Computational studies of the early intermediates of the bacteriorhodopsin photocycle

Michael Engels [a], Klaus Gerwert [b], Donald Bashford [a,*]

[a] *The Scripps Research Institute, Department of Molecular Biology, La Jolla, CA 92037, USA*
[b] *Ruhr-Universität Bochum, Institut für Biophysik, Postfach 102148, 44780 Bochum, Germany*

Abstract

Starting from a refined model of bacteriorhodopsin's ground state, alternative models of the K and L intermediates with retinal in either 13-*cis* or 13-14-*dicis* configuration have been generated by molecular dynamics simulations. All models have been submitted to electrostatic calculations in order to determine the $pK_{1/2}$ values of particular residues of interest in the active site. Our $pK_{1/2}$ calculations for the refined ground state can reestablish our former results, this time without adjusting the intrinsic pK of the Schiff base. For the K intermediate the electrostatic calculations show no significant change in the $pK_{1/2}$ values compared to the ground state for most of the titrating groups in the active site. For the L intermediate where retinal possesses a 13-*cis* configuration, we found that electrostatic factors decrease the $pK_{1/2}$ value of the Schiff base by 4–5 pK-units compared to the ground state. The calculations suggest that changes of the electrostatic environment via a pure 13-*cis* model are sufficient to produce a pK reduction of the Schiff base that will promote subsequent proton transfer steps.

Keywords: Bacteriorhodopsin; Intermediates: Electrostatic; Molecular dynamics simulation; Titration; Proton pump

1. Introduction

The pump action of bacteriorhodopsin (bR) involves the protonation and deprotonation of various titrating groups inside the membrane protein [1–3]. Structural changes of the Schiff base and in the protein moiety accompany or precede these protonation changes. Our aims are to understand the energetics of proton transfer, the conformational changes during the photocycle and the interplay between conformational change and proton transfer.

The method of molecular dynamics (MD) simulations has been used in order to refine the present structural model of bR's ground state and to generate structural models of some of the intermediates of bR's photocycle. In particular, we have applied these techniques to simulate the transition of the retinal from all-*trans* to 13-*cis* or from all-*trans* to 13,14-*dicis* to generate possible K-like and L-like intermediate structures.

So far the structure of bR provided by Henderson et al. [4] is limited to the part of the protein immersed in the membrane. Likewise our knowledge of bR's pump mechanism refers for the most part to the central region of the membrane protein. For the early steps of the photocycle it can be expected that

* Corresponding author.

SSDI 0301-4622(95)00020-8

structural changes or changes in the protonation states of titrating groups (such as the tranfer of a proton from the Schiff base to Asp-85 in the L to M transition) are confined to this region. In applying this assumption to our dynamics simulations we focused on the central part of bR. Water molecules have been included explicitly in this part of the membrane protein. The effect of the peripherical regions of bR have been calculated by more approximate methods, as described below.

Electrostatic calculations using a quasi-macroscopic model can provide estimates of the $pK_{1/2}$ values of titrating groups in proteins and have been applied successfully to bacteriorhodopsin [5,6]. Here we apply these methods to the calculation of the refined model of the ground state and to the structural models of the K and L intermediates of bR's photocycle.

2. Modelling the initial structure

All calculations have been based on the structure provided by Henderson et at. [4], modified by shifting the D helix 3 Å towards the cytoplasmic side as suggested by Henderson (personal communication). Arg-82 has been reoriented towards the Schiff base and is part of the counter-ion complex, as in our earlier work [5].

Interhelical loops not included in the Henderson model have been introduced in our model of bR. For the relatively short loops (A–B, C–D, D–E, and E–F) coordinates have been constructed using a fragment data approach implemented in standard molecular modelling software [7]. For the longer loops a helical conformation was assumed at the beginning of the modelling procedure but subsequent minimization and equilibration led to a strong distortion of these elements. The C-terminus of the G-helix has been extended by three residues assuming a helical conformation for this part. The resulting structure has been equilibrated over 20 ps using MD simulations at 1000 K and finally energy minimized. During this whole loop building procedure the part of the structure provided by Henderson et al. [4] was kept rigid. The resulting model served as starting structure for all following simulations of the ground state.

3. Molecular dynamics simulation of the ground state

The dynamics simulations employed the stochastic boundary molecular dynamics method [8,9] implemented in the program CHARMM22 [10] limiting the fully detailed simulation to the central region of the protein. An ellipsoidal region with principal axes a, b, and c in the x, y, and z directions, respectively, ($a = 8.5$ Å, $b = 17.0$ Å, and $c = 26.0$ Å) around the geometric center of the protein defined the full simulation region. A total of 1672 protein atoms including all residues of the active site as well as the whole chromophore lie inside this region. Protein atoms outside this region were treated by Langevin dynamics to approximate the thermal and frictional effects of the surrounding bath. In addition, these atoms experience mean boundary forces which contribute to the structural integrity of the protein. These mean forces are represented as linear forces with force constants derived from the atomic mean-square fluctuation [9]. This scheme keeps the structure close to the coordinates modelled from cryo-electron microscopy data and reduces the distorting effect of the vacumm on the outside of the structure [11] while giving maximum flexibility to that region where the significant structural changes are supposed to take place.

107 TIP3P [12] water molecules have been added to the ellipsoidal region according to sterical criteria using a protocol suggested by Brooks and Karplus [9] approximating water molecules as a sphere with a diameter of 2.75 Å. Less than the half of these water molecules are placed inside the membrane protein. The other half cover parts of the cytoplasmic and extracellular surfaces. After the placement of the water molecules the system was again energy minimized and finally equilibrated over 20 ps holding the protein atoms on their original position by a restor-

Table 1
rms deviation in [Å] of side chains of particular interest from the starting position. The values are averages over the last 10 ps of either simulation

MD-run	D85	D212	R82	D96	D115	Schiff base
BR_{C22}	1.2	0.8	1.4	0.8	2.1	1.1
BR_{C22hb}	1.1	0.8	1.4	1.0	1.3	1.3

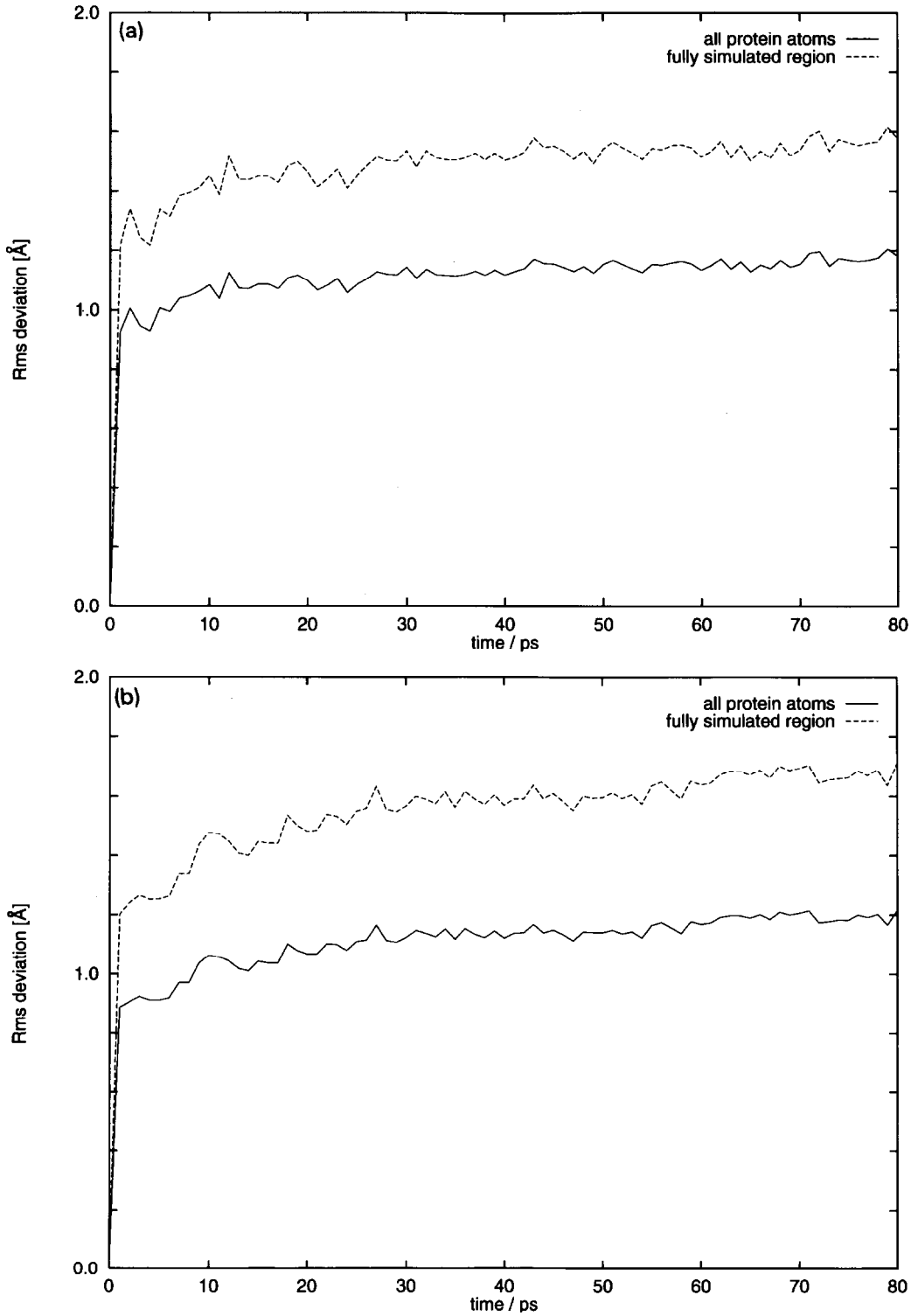

Fig. 1. Rms deviation from the starting structure of all protein atoms (continuous line) and of those proteins atoms lying inside the unrestrained region during the dynamics runs BR_{C22} (a) and BR_{C22hb} (b).

ing force (force constant $k_f = 0.083$ kcal/mol Å^2 times atomic mass).

The final MD simulations were carried out at 300 K over 80 ps using the all-atom force field version 22 (MacKerell, manuscript in preparation) of the CHARMM program. There were no restraints on any atoms inside the ellipsoid. In a second series of dynamics runs we employed, in addition, an H-bond potential. Water molecules were free to move between the fully simulated region and the part treated by Langevin dynamics. Their evaporation was hindered by a deformable boundary force according to the method of Brooks and Karplus [13].

Parameters and charges for the protonated Schiff base of retinal are according to Tavan et al. [14], its dihedral angle force constants are according to Humphrey et al. [15]. The protonation state of titrating groups inside the simulation region are as given in the standard CHARMM topology, except for Asp-96 and Asp-115 which are assumed to be protonated [2,3]. In order to model the shielding effect of the solvent, the net charge of titrating groups outside the ellipsoidal region have been neutralized.

Fig. 1a and b show the root mean square (rms) deviation of all protein atoms and of those inside the fully simulated region from their starting structure for the simulation runs BR_{C22} and BR_{C22hb}, where BR_{C22} refers to the 80 ps simulation without using any additional H-bond term; and BR_{C22hb} refers to the 80 ps MD simulation with an additional H-bond term.

As expected, the deviation of the atoms lying in the unrestrained region is higher than the overall deviation, but at 1.7 Å still well below of that former MD simulations [16,17]. The rms deviations for side chains of particular interest (averaged over the last 10 ps of the runs) are listed in Table 1.

In the 80 ps MD run performed with an additional H-bond potential, one water molecule invaded the active site of bR covering a distance of almost 7 Å. Its original position had been between the C and D helices close to Asp-85. This water molecule links the carboxylate functions of Asp-85 and Asp-212 and the Schiff-base proton via H-bonds (see Fig. 2); but in the 80 ps MD run using the default CHARMM22 force field such behavior was not observed. Instead the Schiff-base proton is within H-bond distance of Asp-212 but the angle between the carboxylate group of Asp-212 and the Schiff-base proton (90 degrees) suggests almost no or a very weak H-bond (see Fig. 3). In both MD runs Asp-85 is H-bonded to one water molecule and to the guanidinium group of Arg-82. A direct interaction of Asp-85 with the Schiff-base proton via H-bonding did not occur.

In both runs the carboxylate groups of Asp-96 and the carbonyl function of Lys-216 are both connected to a chain of water molecules which extends to the cytoplasmic surface. As a consequence of the reorientation of Arg-82 towards the Schiff base a continuous line of water molecules is also found at the extracellular side making H-bonds to Asp-212 and Tyr-57 and extending to the extracellular surface. Single water molecules are also found close to the β-ionone ring systems of the retinal.

4. Modelling the K and L states

The equilibrated structure of the BR_{C22} run served as the starting structure for two series of MD simulations in which the retinal chromophore has been isomerized either to 13-*cis* or 13,14-*dicis*. The default CHARMM force field was used for these simulations and the partitioning of the system into a fully simulated region and a restrained surrounding has been sustained. Isomerization of the retinal was accomplished using the method of Nonella et al. and parameters of Zhou et al. [16] in which the torsional potential for the 13–14 bond is abruptly changed to produce the 13-*cis* isomerization, or both the 13–14 and 14–15 bonds to produce the 13,14-*dicis* isomerization. Both simulations were carried out for 40 ps (experimentally the J intermediate relaxes to K on a 3-ps time scale [18]). We call the resulting model of the intermediate with the chromophore in 13-*cis* configuration $K_{13\text{-}cis}$ and the other model with retinal in 13,14-*dicis* configuration $K_{13,14\text{-}dicis}$.

The K to L transition takes place on the microsecond time scale, which is beyond the reach of ordinary MD simulations [19]. So in order to reach an L-like state the MD simulations were continued a further 30 ps at elevated temperature (T = 450 K), cooled down to 300 K and equilibrated for a further 40 ps. During the high temperature simulation the water molecules have been held on their original

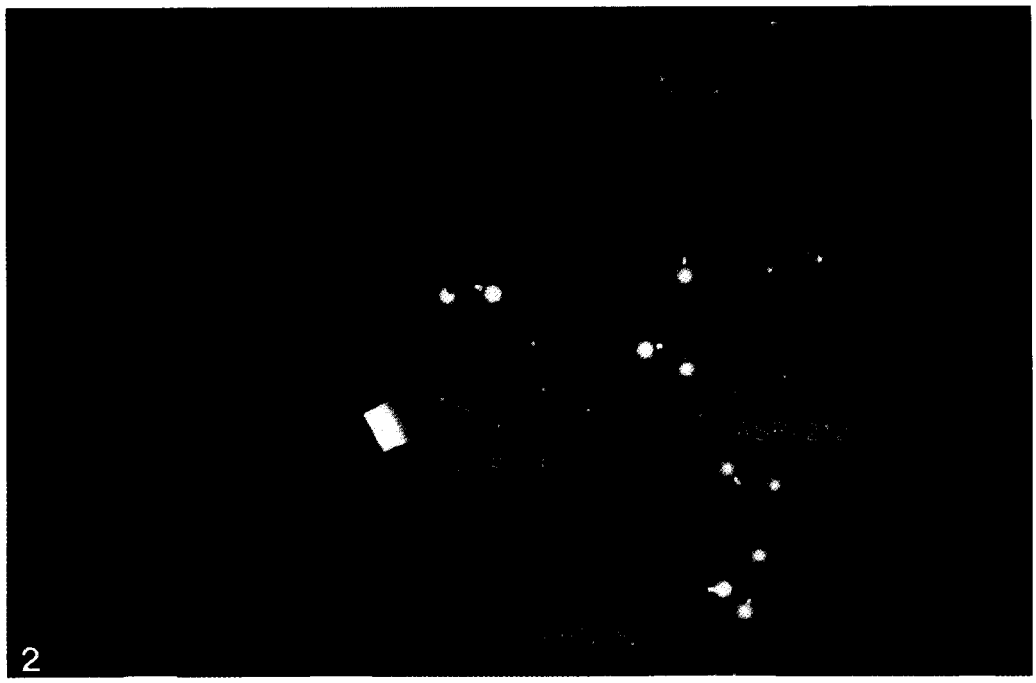

Fig. 2. Detailed view of the retinal binding site showing the final structure after 80 ps MD simulation in the BR_{C22hb} run. The cytoplasmic side is up. The retinal is depicted in green (the nitrogen–proton in blue-white), Asp-85 (left) and Asp-212 in ochre and Arg-82 in red. Note the water molecule inside the active site which is H-bonded to Asp-85, Asp-212 and the Schiff base.

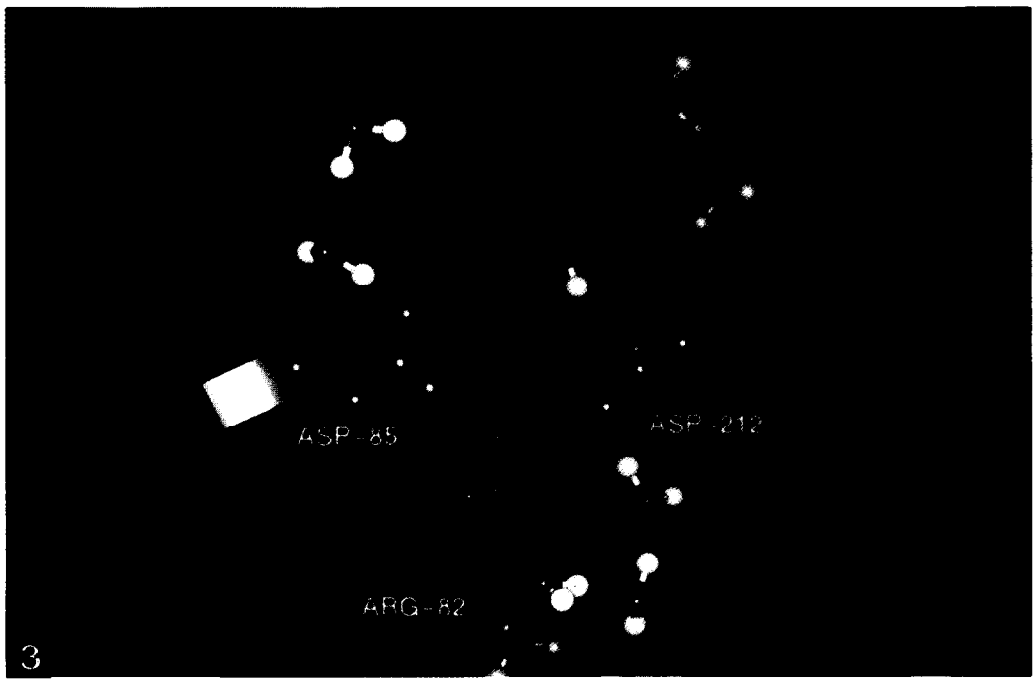

Fig. 3. Detailed view of the retinal binding site showing the final structure after 80 ps of MD simulation in the BR_{C22} run. For the color code see Fig. 2.

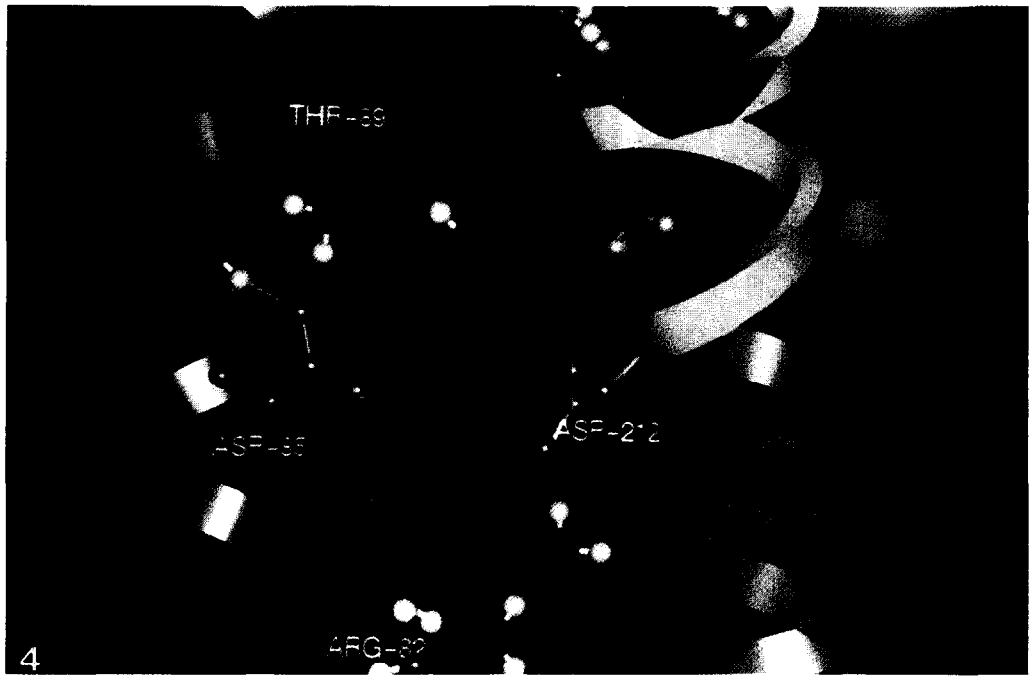

Fig. 4. Detailed view of the retinal binding site in the model $K_{13\text{-}cis}$. For the color code see Fig. 2, in addition Thr-89 is shown in red. Note that the distorted retinal is bridged to Asp-85 by a water molecule although the Schiff-base proton is pointing towards the cytoplasmic side.

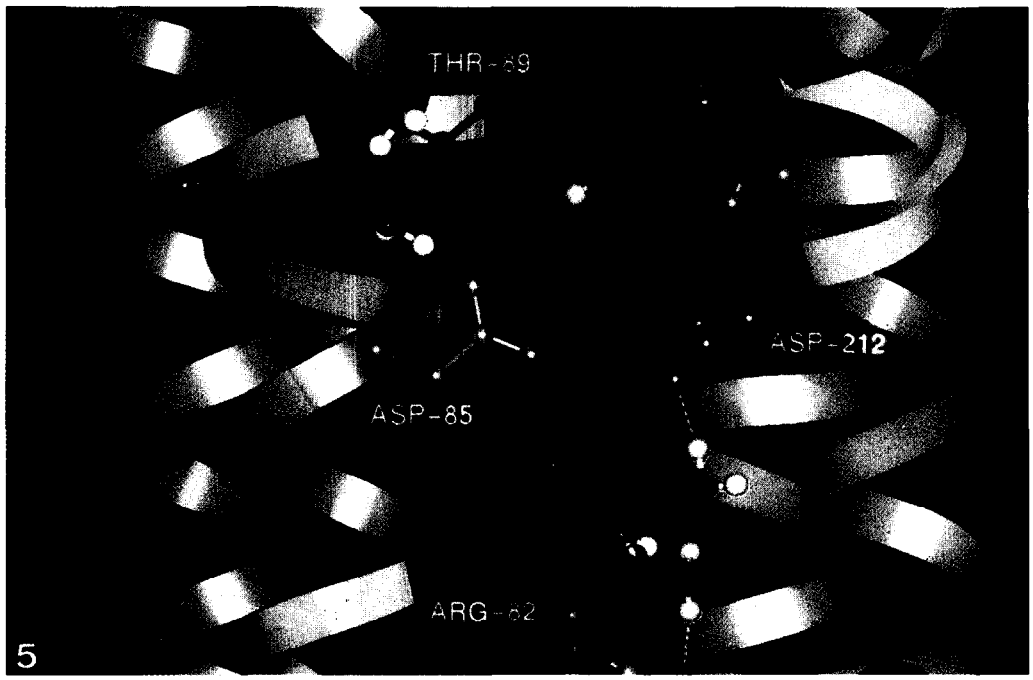

Fig. 5. Detailed view of the retinal binding site in the model $K_{13,14\text{-}dicis}$. For the color code see Figs. 2 and 4.

position by a restraining force. We hypothesize that the resulting structures are L-like intermediates and call them $L_{13\text{-}cis}$ and $L_{13,14\text{-}dicis}$, with the retinal in 13-*cis* and 13-14-*dicis* configuration, respectively.

The resulting isomerization of the retinal from all-*trans* to 13-*cis* or from all-*trans* to 13–14-*dicis* in the K simulation occurred within 0.5 ps in agreement with experimental data [20,21] and recent MD simulations [16]. Both K isomers show a strong twist along their retinal polyene chain which is almost missing in the models of the L intermediate. Detailed pictures of the active site in the $K_{13\text{-}cis}$ and $K_{13,14\text{-}dicis}$ model after their equilibration are shown in Figs. 4 and 5, respectively. An interesting feature of the $K_{13\text{-}cis}$ model is the indirect linkage of the Schiff-base proton with the carboxylate group of Asp-85 via H-bonding with one water molecule. This linkage has also been preserved in the $L_{13\text{-}cis}$ model, but the distance between the Schiff-base proton and the water oxygen increases from 3.0 Å in $K_{13\text{-}cis}$ to 3.7 Å in $L_{13\text{-}cis}$. In $K_{13\text{-}cis}$ the Schiff-base proton is also within H-bonding distance to the hydroxl group of Thr-89. This distance is further decreased in $L_{13\text{-}cis}$. Mutagenesis studies showed that substitution of Thr-89 can decrease the steady-state proton-pump activity by almost 35% and the initial rate proton-pump activity by up to 70% [22]. In $K_{13,14\text{-}dicis}$ (see Fig. 5) the Schiff-base proton is likewise inclined towards Asp-85, but the distance between both groups does not suggest any direct interaction. Asp-85 is H-

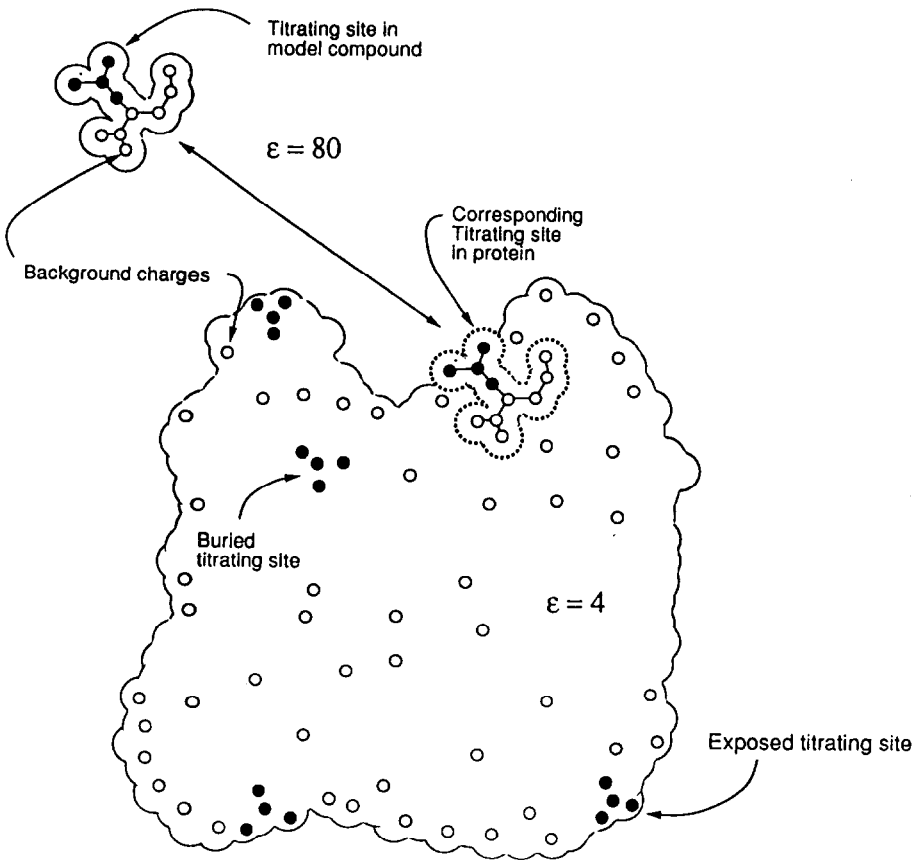

Fig. 6. The macroscopic idealization used for the electrostatic calculaions. The protein and membrane are rigid low-dielectric objects with embedded, permanent charges. Titration is the alteration of charges on a titrating site. The model compound is carved out from the parent protein. $pK_{1/2}$ differences between the protein and model compound are due to differences in the electrostatic work required to make charge alterations in the protein titrating site and the corresponding model compound.

bonded to one water molecule and forms a salt bridge to Arg-82. The distance between the Schiff-base proton and the hydroxyl group of Thr-89 is 3.4 Å, but the angle between the two groups does not imply H-bonding. However, turning the C_α–C_β bond of Thr-89 by 180 degrees brings the hydroxyl group into an H-bond with the Schiff-base proton. In $L_{13,14\text{-}dicis}$ this situation is not preserved because the Schiff-base proton has turned towards Asp-212.

5. Electrostatic calculations and $pK_{1/2}$ values

We use the MEAD (Macroscopic Electrostatics with Atomic Detail) method to calculate the titration behavior of ionizable groups integral to the proton pumping mechanism of bR [4]. The method is based on the assumption that protein, water and membrane each have a uniform dielectric constant and that the detailed shape of the dielectric boundaries and the positioning of charges depend on atomic coordinates, charges, and van der Waals radii. A dielectric value of 4 was assumed for the protein and the membrane, and a dielectric value of 80 was used for the water. In the electrostatic calculations the water molecules introduced in the dynamics simulations have been taken out and the resulting cavities have been treated as a space with a dielectric constant of 80. In addition, the charge states of titrating groups outside the ellipsoidal region have been restored according to the default charges in the CHARMM topology, since the macroscopic method includes solvent screening explicitly.

The differences in the energetics of the titration of groups in the protein versus the same groups in corresponding model compounds is assumed to be purely electrostatic (Fig. 6). The electrostatic terms contributing to $pK_{1/2}$ shifts include the interaction of the titrating group with the polarization that the group itself induces in its surroundings (Born self-energy) and the interaction of the titrating groups with non-titrating polar groups such as the protein backbone (background or dipole interaction energy). These two terms modify the model compound $pK_{1/2}$ to give what Tanford defines as the intrinsic pK, which is the $PK_{1/2}$ a group would have if all other titrating groups were in their neutral states. Finally, we add the interactions between titrating sites and a suitable summation over the possible protonation states of the protein as a whole to calculate the titration behavior of the ionizable groups, some of which will have simple titration curves describable by a single $pK_{1/2}$ value, and some of which will be more complex. The details of this method and the possibility of complex titration curves have been described previously [5].

For the electrostatic calculations we use the computer program suite, MEAD, developed in our lab and available by 'anonymous ftp' from ftp.scripps.edu:/pub/electrostatic.

As previously reported by us [5], and by Sampogna and Honig [6] the calculated $pK_{1/2}$ values are

Table 2
Calculated $pK_{1/2}$ values for the titrating sites in the structural models HE, BR_{C22}, BR_{C22hb}, $K_{13\text{-}cis}$, $K_{13,14\text{-}dicis}$, $L_{13\text{-}cis}$, and $L_{13,14\text{-}dicis}$ integral to its proton pump action. "Prot." means that the titrating group is protonated over the whole pH range of interest. HE represents the energy minimized structure of Henderson et al. [4] without loops, the D-helix shifted and Arg-82 pointing towards the active site, BR_{C22} and BR_{C22hb} refer to the models of the ground state using different MD force fields, $K_{13\text{-}cis}$ and $K_{13,14\text{-}dicis}$ to the models of the K intermediate, and $L_{13\text{-}cis}$ and $L_{13,14\text{-}dicis}$ to the models of the L intermediates

Site	HE	BR_{C22}	BR_{C22hb}	$K_{13\text{-}cis}$	$K_{13,14\text{-}dicis}$	$L_{13\text{-}cis}$	$L_{13,14\text{-}dicis}$
Asp-85	−3.3	−0.3	1.9	−1.6	0.0	−1.0	−0.5
Asp-96	8.8	9.0	8.3	10.1	6.8	16.3	8.2
Asp-115	9.2	8.5	10.2	8.0	10.0	9.0	8.3
Asp-212	−13.3	−10.7	−9.9	−12.2	−11.3	−12.9	−8.4
Tyr-57	prot.	prot.	prot.	prot.	prot.	prot.	prot.
Tyr-185	prot.	prot.	prot.	prot.	prot.	prot.	prot.
Arg-82	prot.	prot.	prot.	prot.	prot.	prot.	prot.
Schiff base	17.4	14.8	13.2	14.8	17.2	9.4	19.2

consistent with the experimentally determined protonation states of the sidechains in the ground state [1–3,23–29]. It should be mentioned that the pK_{int} of the Schiff base has not been adjusted as it was in our previous investigation [5]. Table 2 shows that both Asp-85 and Asp-212 are found to the deprotonated at physiological pH with the tendency that Asp-85 is protonated first when the pH is decreased, in agreement with the experiment. Asp-96 and Asp-115 are predicted to be protonated at physiological conditions [2] as are Tyr-57, Tyr-185 and Arg-82. The unusually high or low $pK_{1/2}$ of some residues, for instance Tyr-185, Tyr-57, and Asp-212, suggests that these groups could be involved in conformational transitions taking place upon protonation or deprotonation.

For the two models of the K intermediate, the protonation pattern almost matches that of the ground state. The most obvious difference in the electrostatic calculations of the K intermediate is the relatively low $pK_{1/2}$ of Asp-96 in model $K_{13,14\text{-}dicis}$ (with 6.8). In both models of the L-intermediate, however, the $pK_{1/2}$ of Asp-96 is high.

The most interesting outcome of the L calculations is that in $L_{13\text{-}cis}$ the $pK_{1/2}$ of the Schiff base is reduced by 4–5 pK-units compared to the ground state. This suggests that in a pure 13-*cis* model of the photocycle, changes in the electrostatic environment alone are sufficient to substantially lower the Schiff base pK — a necessary prerequisite for the transfer of a proton from the Schiff base to Asp-85 in the subsequent L to M transition. For $L_{13,14\text{-}dicis}$, however, the $pK_{1/2}$ is increased by at least 5 pK-units, which suggests that electrostatic factors do not promote proton transfer in the 13–14-*dicis* model. It should be noted, however, that the predicted $pK_{1/2}$ shift only accounts for the purely electrostatic interaction of the fixed partial charges of the Schiff base with its environment. Steric effects and redistribution of charges through the π-orbital system of the polyene chain as shown by Tavan et al. [14], which could alter the intrinsic pK of the Schiff base, are not taken into consideration.

6. Concluding remarks

The work reported here is part of our efforts to apply theoretical methods to bR's pump cycle. In agreement with other authors we observe the importance of including water molecules during simulations [6,15,16]. But instead of placing water molecules manually into the structure, we use standard methods that had been developed for protein–solvent MD simulations [9]. Our simulations of the ground state show a similar picture as presented by Humphrey et al. and Zhou et al. [15,16]: First, water chains pass through the extracellular and cytoplasmic domain connecting residues which are of importance for the proton pumping process. Second, the configuration of the active site is stabilized by the interaction with the water molecules.

A main question of interest is how the detailed structure of bacteriorhodopsin changes in order to accomplish the proton pumping. As a first step, we have combined molecular modelling and MD simulation with electrostatic calculations. The advantage of this approach is that the electrostatic calculations help to assess the validity of the MD-generated models, which are of uncertain accuracy. The simulated structures, especially for the 13-*cis* model, are consistent with spectroscopic and experimental data, however, they show just one out of many possible choices.

Acknowledgement

The authors are grateful for the support of fellowships by the Deutsche Forschungsgemeinschaft [En 285/1-1] (M.E.) [En 599/7-1] (K.G.) and by the National Institutes of Health [GM45607] (D.B.).

References

[1] M.S. Braiman, T. Mogi, T. Marti, L.J. Stern, H.G. Khorana, and K.J. Rothschild, Biochemistry, 27 (1988) 8516–8520.
[2] K. Gerwert, B. Hess, J. Soppa, and D. Oesterhelt, Proc. Natl. Acad. Sci. USA, 86 (1989) 4943–4947.
[3] K. Gerwert, G. Souvignier, and B. Hess, Proc. Natl. Acad. Sci. USA, 87 (1990) 9774–9778.
[4] R. Henderson, J.M. Baldwin, T.A. Ceska, F. Zemlin, E. Beckmann and K.H. Downing, J. Mol. Biol., 213 (1990) 899–929.
[5] D. Bashford and K. Gerwert, J. Mol. Biol. 224 (1992) 473–486.
[6] R.V. Sampogna and B. Honig, Biophys. J., 66 (1994) 1341–1352.

[7] InsightII, version 2.3.0, Biosym Technologies, San Diego (1993).
[8] A.T. Brunger, C.L. Brooks and M. Karplus, Proc. Natl. Acad. Sci. USA, 82 (1985) 8458–8462.
[9] C.L. Brooks and M. Karplus, J. Mol. Biol., 208 (1989) 159–181.
[10] B.R. Brooks, R.E. Bruccoleri, B.D. Olafson, D.J. States, S. Swaminathan, and M. Karplus, J. Comp. Chem., 4 (1983) 187–217.
[11] W.L. van Gunsteren and A.E. Mark, Eur. J. Biochem., 204 (1992) 947–961.
[12] W.L. Jorgensen, J. Chandrasekhar, J.D. Madura, R.W. Imprey and M.L. Klein, J. Chem. Phys., 79 (1983) 926–935.
[13] C.L. Brooks and M. Karplus, J. Chem. Phys., 79 (1983) 6312–6325.
[14] P. Tavan, K. Schulten and D. Oesterhelt, Biophys. J., 47 (1985) 415–430.
[15] W. Humphrey, I. Logunov, K. Schulten and M. Sheves, Biochemistry, 33 (1994) 3668–3678.
[16] F. Zhou, A. Windemuth and K. Schulten, Biochemistry, 32 (1993) 2291–2306.
[17] M. Nonella, A. Windemuth and K. Schulten, Photochem. Photobiol., 54 (1991) 937–948.
[18] H.-J. Polland, M.A. Franz, W. Zinth, W. Kaiser, E. Kolling and D. Oesterhelt, Biophys. J. 49 (1986) 651–662.
[19] Y. Shichida, S. Matuoka, Y. Hidaka and T. Yoshizawa, Biochim. Biophys. Acta, 723 (1983), 240.
[20] J. Dobler, W. Zinth, W. Kaiser and D. Oesterhelt, Chem. Phys. Lett., 144 (1988) 215–220.
[21] R. Mathies, C. Cruz, W. Pollard and C. Shank, Science, 240 (1988) 777–779.
[22] T. Marti, H. Otto, S, Mogi, S.J. Rosselet, M.P. Heyn and H.G. Khorana, J. Biol. Chem., 266 (1991) 6919–6927.
[23] S. Druckmann, M. Ottolenghi, A. Pande, J. Pande and R.H. Callender, Biochemistry, (21) (1982) 4953–4959.
[24] M. Engelhardt, K. Gerwert, B. Hess, W. Kreutz and W. Siebert, Biochemistry, 24 (1985) 400–407.
[25] K. Gerwert, U.M. Ganter, F. Siebert and B. Hess, FEBS Lett. 213 (1987) 39–44.
[26] A. Lewis, M.A. Marcus, B. Ehrenberg and H. Crespi, Proc. Nat. Acad. Sci. USA, 75 (1978) 4642–4646.
[27] A.G. Doukas, A. Pande, T. Suzuki, R.H. Callendar, B. Honig and M. Ottolenghi, Biophys. J., 33 (1981) 275–280.
[28] S. Subramaniam, T. Marti and H.G. Khorana, Proc. Nat. Acad. Sci. USA, 87 (1990) 1013–1017.
[29] J. Herzfeld, S.K. Das Gupta, M.R. Farrar, G.S. Harbison, A.E. McDermott, S.L. Pelletier, D.P. Raleigh, S.O. Smith, C. Winkel, J. Lugtenburg and R.G. Griffin, Biochemistry, 29 (1990) 5567–5574.